Published in final edited form as:

Neuron. 2014 January 22; 81(2): 349–365. doi:10.1016/j.neuron.2013.12.002.

Age-Dependent Decrease in Chaperone Activity Impairs MANF Expression, Leading to Purkinje Cell Degeneration in Inducible SCA17 Mice

Su Yang[1], **Shanshan Huang**[1,2], **Marta A. Gaertig**[1], **Xiao-Jiang Li**[1,2,*], and **Shihua Li**[1,*]

[1]Department of Human Genetics, Emory University School of Medicine, 615 Michael Street, Room 355, Atlanta, GA 30322, USA

[2]State Key Laboratory of Molecular Developmental Biology, Institute of Genetics and Developmental Biology, Chinese Academy of Sciences, Beijing, China

SUMMARY

Although protein-misfolding-mediated neurodegenerative diseases have been linked to aging, how aging contributes to selective neurodegeneration remains unclear. We established spinocerebellar ataxia 17 (SCA17) knockin mice that inducibly express one copy of mutant TATA box binding protein (TBP) at different ages by tamoxifen-mediated Cre recombination. We find that more mutant TBP accumulates in older mouse and that this accumulation correlates with age-related decreases in Hsc70 and chaperone activity. Consistently, older SCA17 mice experienced earlier neurological symptom onset and more severe Purkinje cell degeneration. Mutant TBP shows decreased association with XBP1s, resulting in the reduced transcription of mesencephalic astrocyte-derived neurotrophic factor (MANF), which is enriched in Purkinje cells. Expression of Hsc70 improves the TBP-XBP1s interaction and MANF transcription, and overexpression of MANF ameliorates mutant TBP-mediated Purkinje cell degeneration via protein kinase C (PKC)-dependent signaling. These findings suggest that the age-related decline in chaperone activity affects polyglutamine protein function that is important for the viability of specific types of neurons.

INTRODUCTION

Aging is a complex biological process and a known primary risk factor for neurodegenerative diseases caused by protein misfolding, such as Alzheimer's disease, Parkinson's disease, Huntington's disease, and other polyglutamine (polyQ)-expansion-mediated diseases that frequently occur in the middle or late stages of life. The misfolded proteins are known to accumulate with age in neuronal cells, and this accumulation increases the level of toxic forms of proteins that can induce neurodegeneration. Aging is also linked to several pathological pathways, including mitochondria dysfunction (Passos and von

*Correspondence: xli2@emory.edu (X.-J.L.), sli@emory.edu (S.L.).

SUPPLEMENTAL INFORMATION

Supplemental Information includes Supplemental Experimental Procedures and seven figures and can be found with this article online at http://dx.doi.org/10.1016/j.neuron.2013.12.002.

Zglinicki, 2005), reactive oxygen species damage (Afanas'ev, 2010), and protein homeostasis disturbance (Akerfelt et al., 2010), which are implicated in neurodegenerative diseases.

Given that neurons are terminally differentiated cells that do not divide, it remains unclear whether aging-related factors promote the accumulation of mutant proteins in neurons versus the greater length of time proteins are expressed or whether aged neurons are more vulnerable to misfolded proteins versus the cumulative effects of misfolded proteins with age. Understanding the mechanisms underlying age-dependent neurodegeneration is critical if we are to develop effective therapeutics for protein-misfolding-mediated neurodegenerative diseases. For example, if aged neurons are more vulnerable to misfolded proteins than young neurons, then reversing aging-related cellular dysfunction would be more effective than reducing the expression of polyQ proteins in treating these neurodegenerative diseases, especially given that proteins with expanded polyQ repeats may still preserve critical function (Cattaneo et al., 2005).

Unfortunately, sorting out these important issues is difficult using current genetic mouse models of neurodegenerative diseases. This is because most of these mouse models express mutant proteins throughout life, making it difficult to distinguish between the cumulative effects of mutant proteins on neuronal cells over time versus a greater vulnerability of aged neurons to mutant proteins. To remedy this, we established an inducible mouse model of spinocerebellar ataxia 17 (SCA17) that allows for the expression of mutant proteins at different ages, enabling us to examine whether and how aged neurons are particularly affected. SCA17 is caused by polyQ expansion in the TATA box binding protein (TBP), a transcription factor essential for the expression of most genes. Despite the critical function of TBP, in SCA17 patients, expansion of the polyQ (>42 glutamines) in TBP results in late-onset neurological symptoms, including ataxia, rigidity, dystonia, and dementia (Bruni et al., 2004; Rolfs et al., 2003; Toyoshima et al., 2004); this polyQ expansion also causes age-dependent neurodegeneration in the same manner as the other eight polyQ diseases, among them Huntington's disease (Orr and Zoghbi, 2007). These facts suggest that the neuronal toxicity of mutant TBP and other polyQ disease proteins depends on aging-related factors. Because TBP is a well-characterized transcription factor, SCA17 makes an ideal model for investigating how polyQ-expansion-mediated protein misfolding causes neuronal degeneration in an age-dependent manner.

Using our SCA17 knockin (KI) mouse model, we induced mutant TBP expression in mice at different ages. We found that SCA17 disease phenotypes in older mice progress much faster, along with decreases in chaperone activity and Hsc70 level. In addition, mesencephalic astrocyte-derived neurotrophic factor (MANF), a protein with a neuroprotective effect, is down-regulated in the cerebellum, especially in the Purkinje cell layer, in the presence of mutant TBP. Mutant TBP binds weakly to the transcription factor XBP1s and mediates less MANF transcription, which can be reversed by Hsc70 overexpression. Overexpression of MANF by lentiviral vector infection and transgenic mouse approach ameliorates toxicity caused by mutant TBP in Purkinje cells in SCA17 mice. MANF upregulates protein kinase C (PKC) phosphorylation and reverses reduced PKC phosphorylation in the cerebellum of SCA17 mice. These findings indicate that age-related decrease in chaperone function could

cause the accumulation of mutant TBP and reduce its normal function on MANF transcription, contributing to the selective neurodegeneration in SCA17.

RESULTS

Generation of Inducible SCA17 KI Mice

We previously established floxed TBP105Q mice in which a transcription stop codon is used to prevent the transcription of mutant TBP (Huang et al., 2011) (Figure 1A). To induce the expression of mutant TBP in mice at different ages, we crossed floxed heterozygous TBP105Q mice with CreER transgenic mice that express a fusion protein containing Cre recombinase and an estrogen receptor ligand binding site under the control of chicken β-actin promoter. Upon intraperitoneal injection of tamoxifen, an estrogen receptor ligand, this ligand can bind Cre recombinase fusion protein and cause it to enter the nucleus and act on the loxP sites, resulting in the removal of the stop codon and the expression of mutant TBP (Figure 1A). For simplicity, the mice carrying both the floxed TBP105Q gene and CreER transgene are referred to as TBP105Q inducible KI mice. Littermates with other genotypes, including CreER transgenic mice, heterozygous TBP105Q floxed mice, and wild-type (WT) mice, were used as control mice, given that the injection of tamoxifen in these mice does not lead to the expression of mutant TBP. Thus, tamoxifen can be injected into KI mice at different ages in order to permanently induce mutant TBP expression throughout the body.

First, we injected tamoxifen in 3-month-old TBP105Q inducible KI mice for 5 consecutive days. Different tissues were collected for western blot analysis 2 months after the last injection. Soluble mutant TBP in the cortex and liver of injected KI mice was seen in western blots probed with 1C2 antibody, which recognizes the expanded polyQ region. Immunoprecipitation of mouse TBP with the rabbit polyclonal antibody EM192 verified the existence of soluble mutant TBP in the cortex and liver (Figure 1B). Western blot probed with 1TBP18 antibody, which preferentially reacts with aggregated forms of mutant TBP, revealed SDS-insoluble mutant TBP aggregates in the stacking gel, which were from the cerebellum, cortex, and muscle of KI mice (Figure 1C). Immunohistochemistry with 1C2 antibody also verified the presence of mutant TBP in different brain regions in KI mice 2 months after tamoxifen injection at the ages of 3 or 14 months. Nuclear staining of mutant TBP was evident in the cortex, striatum, hippocampus, and cerebellum of these KI mice (Figure 1D, left). Staining with 1TBP18 antibody revealed small mutant TBP aggregates in the nucleus under high magnification (1003) (Figure 1D, right). All these results confirm that tamoxifen injection can induce the expression of mutant TBP in the brain and peripheral tissues at different ages.

Aging Exacerbates Neurological Phenotypes and Purkinje Neuron Degeneration in TBP105Q Inducible KI Mice

To study the impact of aging on SCA17 disease progression in our TBP105Q inducible KI mouse model, KI mice at 3, 9, and 14 months of age were injected with tamoxifen for 5 days and then examined on a weekly basis for 3 months or until death. After tamoxifen injection, KI mice gradually developed characteristic SCA17 disease phenotypes, such as reduced body weight, impaired motor function, and hunched-back appearance (Figure 1E–1G). Some

14-month-old mice died starting from 40 days after tamoxifen injection, but none of the 3-month-old mice died within 3 months after injection. Because some mice had been sacrificed in order to examine brain pathology and TBP expression at different times after injection, the loss of body weight of these mice was used to reflect disease severity, given that body weight can also be more reliably quantified than other behavioral phenotypes. In comparison to the age-matched controls, older KI mice displayed a significant loss of body weight at an earlier time after tamoxifen-induced expression of mutant TBP; for example, 14-month-old KI mice started to lose their body weight significantly at 35 days after injection, whereas the 9-month-old group of KI mice showed a significant weight loss at 53 days after injection. On the other hand, 3-month-old KI mice showed no obvious body weight reduction until 113 days after injection (Figure 1E). Comparing KI mice at different ages also showed that older KI mice lost more body weight than younger KI mice (Figure 1F). Consistently, a hunched-back appearance of 3-, 9-, and 14-month-old KI mice was seen at 130, 75, and 60 days after tamoxifen injection, respectively (Figure 1G). We also analyzed rotarod performance to measure the motor function of KI mice. In agreement with the loss of body weight result, 14-month-old KI mice had the worst performance, given that the time they stayed on a rotating rod was significantly shorter than the age-matched controls, and this motor function deficiency started earlier (day 9 after tamoxifen injection) than in 3- and 9-month-old KI mice (day 15 after injection) (Figure 2A). The oldest KI mice (14 months old) also had poorer rotarod performance than the younger (3- and 9-month-old) KI mice (Figure 2B). To further characterize the motor deficit, 1.5 months after tamoxifen injection, KI mice at different ages were subjected to balance beam assay. The performance of 3-month-old KI mice was comparable to age-matched controls, whereas 14-month-old KI mice took a significantly longer time to walk through the beam, suggesting an age-related decline in motor coordination and activity (Figure 2C). Ataxia is a definitive phenotype of SCA17 and results in gait abnormality. Using a foot-printing assay, we found that gait abnormality was most apparent in 14-month-old KI mice (Figure S1A available online), given that the stride length of 14-month-old KI mice was significantly decreased in comparison to 3- and 9-month-old KI mice (Figure S1A and S1B).

Next, we wanted to correlate the phenotypes observed in KI mice with Purkinje neuron degeneration, a characteristic neuropathological feature seen in both SCA17 patients (Rolfs et al., 2003) and previously established SCA17 mouse models (Friedman et al., 2007; Huang et al., 2011). In comparison to 16-month-old WT mice, immunostaining with an antibody to calbindin, a specific marker protein for Purkinje cells, revealed that the 14-month-old KI mice had the most severe Purkinje neuron loss after 2 months of tamoxifen injection, given that the molecular layer thickness and dendritic branches were also significantly decreased; the 9-month-old KI mice had a modest level of degeneration, whereas the Purkinje neurons in the 3-month-old group remained largely intact (Figures 2D, 2E, and S1C). Furthermore, these results were confirmed by conventional Nissl and Golgi staining (Figure S1D and S1E). Western blot analysis of the ratio of calbindin to actin in the cerebellum of KI mice at different ages also verified that the older KI mice showed greater loss of Purkinje cells after turning on the expression of mutant TBP by tamoxifen injection (Figures 2F and 2G). Because the tamoxifen induction time was the same for KI mice at different ages, all these

results unequivocally suggest that aging accelerates the disease progression and neurodegeneration in our SCA17 KI mouse model.

Aging Promotes Mutant TBP Accumulation in TBP105Q Inducible KI Mice

In order to assess whether aging influences the expression levels of mutant TBP, we used western blots to examine the levels of SDS soluble mutant TBP, because mounting evidence suggests that, in polyQ disease models, soluble mutant protein is more pathogenic than aggregated proteins (Nagai et al., 2007; Takahashi et al., 2008). There were higher levels of mutant TBP in the cortex and the cerebellum of 9- and 14-month-old KI mice than 3-month-old KI mice 3 months after tamoxifen induction (Figures 3A and 3B). However, semiquantitative RT-PCR showed similar amounts of mutant TBP transcripts in 3- and 9-month-old KI mice after tamoxifen injection (Figures 3C and 3D), suggesting that mutant TBP tends to accumulate in aged neurons at the protein level. Consistent with our previous transgenic mouse model (Friedman et al., 2007), there is a reduced amount of WT TBP protein in the presence of mutant TBP (Figures 3E and 3F). To rule out the possibility that the reduced WT TBP protein is due to only one functional allele of WT TBP in KI mice, we compared WT TBP level in KI mice with or without tamoxifen injection. WT TBP was only decreased when mutant TBP was induced after KI mice were injected with tamoxifen (Figure S1F), suggesting that the total amount of TBP is tightly regulated and that the expression of mutant TBP can down-regulate WT TBP, presumably because of the critical functions of TBP.

Aging Decreases Chaperone Activity and Hsc70 Levels in Mouse Brain

There are three major cellular mechanisms for coping with mis-folded proteins accumulated in the brain: the chaperone system, the ubiquitin-proteasome system (UPS), and the autophagy system (Gestwicki and Garza, 2012; Li and Li, 2011). Several studies already implicate aging in impaired UPS activity in the CNS (Keller et al., 2000), but whether aging affects autophagy and chaperone function remains to be fully investigated. First, we checked autophagy activity in the cortex and cerebellum of 3-, 12-, and 21-month-old WT mice by measuring the level of LC3B, a component of autophagosomes, and p62/SQSTM1, a polyubiquitin binding protein degraded by autophagy. We saw no detectable differences of either LC3B or p62 between different ages (Figure 4A), suggesting that autophagy activity in the brain is not significantly impacted by aging, at least under unstressed conditions.

Next, we focused on the chaperone system, which consists of a large family of proteins. To measure chaperone, we adopted an in vitro luciferase protection assay activity (Thulasiraman and Matts, 1998) in which brain lysate and recombinant luciferase were mixed together and incubated at a denaturing temperature (42°C). At this temperature, the luciferase is thermally unstable and tends to misfold, whereas the chaperones in the brain lysates can prevent misfolding and maintain the luciferase activity. With chaperone inhibitor PU-H71 added into the mixture as a control, the specific chaperone activity could be quantified (Figure 4B). We found that the luciferase activity significantly decreased with the lysates from aged cortex and cerebellum (Figure 4C), supporting the idea that chaperone activity declines during aging. Furthermore, we explored which members of the chaperones were responsible for this change. By individually checking each form of the major

chaperones with western blot analysis, we found that the protein levels of Hsc70 and Hsp90 were significantly decreased in the cerebellum of WT mice from 3 to 21 months, whereas Hsp70 and Hsp40 levels remained stable (Figures 4D and 4E). Immunohistochemistry confirmed that Hsc70 level was reduced in the Purkinje cells of 18- and 24-month-old WT mice in comparison to 6-month-old WT mice (Figure 4F). Therefore, the age-related reduction of Hsc70 could explain the weakened luciferase protection and is also likely to accelerate mutant TBP accumulation in aged TBP105Q inducible KI mice.

Age-Related Decrease of Mesencephalic Astrocyte-Derived Neurotrophic Factor Specifically Occurs in the Cerebellum of TBP105Q Inducible KI Mice

Mutant TBP in aged neurons can selectively affect the expression of certain neuronal proteins to cause selective neurodegeneration. To identify such targets, we examined microarray results obtained previously with the cerebellum tissues from our TBP transgenic mice (Friedman et al., 2007). One interesting candidate is MANF, which is alternatively named arginine-rich, mutated in early-stage tumor (ARMET). Emerging evidence argues that MANF plays a potential protective role on neuronal survival (Hellman et al., 2011; Mizobuchi et al., 2007; Voutilainen et al., 2009). Interestingly, we found that MANF was significantly decreased in the cerebellum from 9- and 14-month-old KI mice, which is consistent with increased mutant TBP with age after tamoxifen injection (Figures 5A and 5B). We also checked another neurotrophic factor, BDNF, but found that its level was comparable to WT and KI mice (Figure S2A and S2B). These results suggest that MANF is selectively reduced by mutant TBP. Immunohistochemistry showed that MANF was enriched in the Purkinje cell layer and was lost in 14-month-old KI mice (Figure 5C). However, MANF staining intensity in other brain regions, including the cortex, striatum, and brain stem, was indistinguishable between WT and 14-month-old KI mice (Figure S2C). We performed the same immunostaining of a 12-month-old HdhQ150 KI mouse and saw a clear enrichment of MANF in the Purkinje cell layer (Figure S2D). All these findings indicate that mutant TBP can specifically downregulate MANF in Purkinje cells.

To investigate whether mutant TBP affects the transcription of MANF, we performed semiquantitative PCR. We saw a decreased level of MANF transcripts in the cerebellum of KI mice in which mutant TBP was induced at 9 months of age, but no such decrease was observed in the cortex or cerebellum of KI mice that started to express mutant TBP at 3 months (Figure 5D); the decrease was further verified by quantitative PCR via a real-time PCR assay (Figure 5E). On the basis of these results, we conclude that an age-related and tissue-specific reduction of MANF mRNA underlies the decrease of its protein expression.

Expanded polyQ Disrupts the Interaction between TBP and XBP1s and Impairs the Transcription of MANF

Given that the MANF mRNA level is decreased in the presence of mutant TBP, we reasoned that mutant TBP could impair MANF transcriptional activity. However, no TATA box sequence is present in the MANF promoter region, indicating that TBP regulates MANF transcription via other transcription factors. An endoplasmic reticulum (ER) stress response element (ERSE) located around 150 bp upstream of the MANF transcription initiation site is known to play a critical role in regulating MANF transcription and is recognized by XBP1

(Mizobuchi et al., 2007), a transcription factor that is activated during ER stress and upregulates genes important for protein folding, maturation, and degradation (Lee et al., 2003). The activation of XBP1 involves an unconventional mechanism: an ER transmembrane kinase, IRE1, splices a 26 nt intron from XBP1 mRNA. This splicing event leads to a frameshift, which converts the biologically inactive XBP1u (unspliced) to its active form, XBP1s (spliced) (Yoshida et al., 2001).

We hypothesized that mutant TBP affects XBP1s-mediated MANF expression in aged neurons. Although we have found that Hsc70 and Hsp90 decrease in the aged brain, Hsc70 has been reported to maintain the protein-DNA binding complex for gene transcription (Gehring, 2004; Li et al., 2008; Zeiner et al., 1999). Thus, we wanted to compare the effects of normal and mutant TBP on the binding of XBP1s to the MANF promoter and also to know whether Hsc70 can influence this binding. To explore this, we needed to use cultured cells in order to express different TBP and Hsc70. First, we performed chromatin immunoprecipitation (ChIP) of human embryonic kidney 293 (HEK293) cells that were transfected with XBP1s and TBP (either 13Q or 105Q) constructs (Figure 6A). Anti-FLAG was used to pull down FLAG-tagged XBP1s. DNA was recovered from the pulldown lysates and used as a template for semiquantitative PCR of the MANF promoter. In comparison to TBP13Q, TBP105Q significantly reduced the association of the MANF promoter with XBP1s (Figure 6B).

Earlier literature indicates that TBP and XBP1s are present in the same transcriptional complex (Hetz, 2012). We wanted to know whether mutant TBP shows altered association with XBP1s, which may account for the decreased association of XBP1s with the MANF promoter and whether Hsc70 can improve the function of mutant TBP. To this end, HEK293 cells were transfected with XBP1s and TBP (either 13Q or 105Q) in the absence or presence of Hsc70. Then, transfected XBP1s was precipitated with anti-XBP1. Significantly less TBP105Q than TBP13Q was coprecipitated with XBP1s (Figure 6C), suggesting that polyQ expansion impairs the interaction between TBP and XBP1s. Furthermore, overexpression of Hsc70 greatly increased the level of both TBP13Q and TBP105Q pulled down, indicating that Hsc70 facilitates the association between TBP and XBP1s (Figures 6C and 6D).

To functionally assess the effect of mutant TBP on the transcription of MANF, we generated a luciferase reporter that is expressed under the control of the MANF promoter (−300, ~+2 nt). As a negative control, we also made a mutant promoter by deleting ERSE in the promoter (Figure 6E, top). HEK293 cells were transfected with the MANF reporter in combination with other constructs, and luciferase intensity was measured in order to quantify MANF transcription levels. As expected, the overexpression of XBP1s, rather than XBP1u, dramatically increased luciferase intensity, indicating that XBP1s indeed stimulates MANF transcription (Figure 6E, bottom). Then, we compared the reporter activity when TBP13Q or TBP105Q was presented with XBP1s. Western blotting was used to quantify the expression level of the transfected proteins (Figure 6F). We found that the expression of TBP105Q yielded a lower level of transcription activity, which is consistent with its weaker association with XBP1s. Importantly, coexpression of Hsc70 significantly increased the reporter activity and eliminated the difference between TBP13Q and TBP105Q (Figure 6G).

To examine whether overexpression of Hsc70 can upregulate MANF expression, we used our previously generated PC12 cell lines that stably express either TBP13Q or TBP105Q (Shah et al., 2009). We found that the endogenous level of MANF was decreased in TBP105Q cells. However, transfection of Hsc70 resulted in a significant increase in MANF level (Figure 6H). Similarly, the TBP105Q cell line showed impaired neurite outgrowth in response to nerve growth factor (NGF), but Hsc70 overexpression could significantly reverse this neurite outgrowth deficit (Figure S3A and S3B). Also, overexpression of Hsc70 via adenoviral vector in the cerebellum of KI mice reduced the degeneration of Purkinje cells and increased the levels of MANF in Purkinje cells (Figure S3C and S3D). Altogether, these findings suggest that chaperone activity is critical for maintaining the normal function of mutant TBP and that the age-dependent decrease in its activity leads mutant TBP to lose its normal function and alters gene expression important for neuronal survival.

MANF Overexpression Ameliorates Mutant TBP Toxicity In Vitro and In Vivo

If a decreased MANF level in the cerebellum contributes to Purkinje cell degeneration in SCA17 mice, then overexpression of MANF should alleviate this pathological change. To test this hypothesis, we generated a lentiviral MANF vector in which mouse MANF is linked with ECFP through an F2A sequence and is expressed under the control of the ubiquitin promoter (Figure 7A). When translated, the F2A peptide can be self-cleaved in order to separate MANF and ECFP, and ECFP fluorescence could be an indicator of MANF expression. First, we infected HEK293 cells with MANF lentivirus and detected robust expression of both MANF and ECFP via western blotting (Figure 7B). Then, we infected stable PC12 cell lines that express either TBP13Q or TBP105Q. After NGF stimulation, we found that MANF overexpression could significantly increase the numbers of TBP105Q cells containing long neurites versus control cells (Figures 7C and 7D), which suggests that MANF rescues the neurite outgrowth defect caused by mutant TBP. The PC12 cells expressing mutant TBP are also sensitive to apoptotic stimuli, such as staurosporine treatment (Shah et al., 2009). MTS assay showed that MANF overexpression was able to significantly improve the survival of TBP105Q PC12 cells (Figures 7E and 7F).

Next, we performed stereotaxic injection of lentivirus expressing MANF into the cerebellum of 12-month-old TBP105Q inducible KI mice. MANF lentivirus was injected on the right side of the cerebellum, and the lentivirus expressing GFP alone was injected into the left side as a control. The injected mice were subjected to tamoxifen treatment 1 month later in order to express mutant TBP for another 1.5 months before being examined. Immunofluorescence staining of the cerebellum revealed the expression of ECFP and GFP, which was used to locate the site of virus infection, and calbindin staining was used to visualize Purkinje cells (Figure 7G). In WT mice, both lentiviral MANF- and GFP-infected sides showed a comparable density of Purkinje neurons (Figure 7G). However, in the KI cerebellum, we saw a severe loss of Purkinje neurons caused by mutant TBP in the lentiviral GFP-infected side, and, importantly, the lentiviral MANF-infected side had a significant increase in the number of Purkinje neurons (Figures 7G and 7H), further confirming the protective effect of MANF on mutant TBP toxicity.

Transgenic MANF Expression Alleviates Ataxic Gait and Purkinje Cell Neurodegeneration in SCA17 KI Mice through PKC Signaling Pathway

Injected MANF lentivirus can only infect a limited area of the cerebellum; therefore, it was difficult to see behavioral changes of SCA17 mice after injection. We generated a MANF transgenic mouse model in which the prion promoter was used to drive the expression of MANF that is tagged with human influenza hemagglutinin (HA) at the C terminus (Figure 8A). Western blot (Figure 8B) and immunohistochemistry (Figure S4) with anti-HA tag confirmed that transgenic MANF was widely expressed in the brain of transgenic mice. Using TBP105Q loxP mice, we recently obtained KI mice (SCA17 KI) that expressed mutant TBP105Q from germline and displayed ataxic gait, manifested by significantly shorter strides and poor coordination between forepaws and hindpaws at the age of 6 months. We crossed MANF transgenic mice with these SCA17 KI mice and generated KI/MANF mice that express both mutant TBP and transgenic MANF. At 6 months of age, KI/MANF mice showed significant improvement in foot-printing phenotype (Figure 8C) and clasping phenotypes (Figure S5A and S5B) in comparison to SCA17 KI mice. Quantification of stride lengths in the foot-printing assay and walking time during the balance beam test verified a significant improvement of motor function and coordination of KI/MANF mice (Figure 8D). Western blotting results revealed an upregulation of calbindin levels in the SCA17 KI mouse cerebellum expressing transgenic MANF (Figure 8E). In agreement with this result, immunofluorescent staining showed that transgenic MANF was also protective on Purkinje neuron survival, given that a significantly higher density of Purkinje neurons was seen in the cerebellum of KI/MANF mice in comparison to SCA17 KI mice (Figure 8F). In addition, the thickness of molecular layer and dendritic complexity was also improved in KI/MANF mice (Figures 8G and S5C). It should be noted that a similar amount of mutant TBP was seen in both SCA17 KI and KI/MANF mice (Figure 8E), suggesting that the rescue effect of MANF was not due to a reduced level of mutant TBP but resulted from improving MANF function.

MANF is found to have neurotrophic effects for rescuing apoptotic neurons (Hellman et al., 2011). Using immunostaining with an antibody to activated caspase 3, we found a minimal level of activated caspase 3 in the cerebellum of SCA17 KI and KI/MANF mice (Figure S6), indicating that the primary cause of Purkinje neuron degeneration in SCA17 is not apoptosis. Given that MANF can also bind membrane receptors in order to trigger intracellular signaling (Henderson et al., 2013), we produced His-tagged MANF in bacteria and purified this recombinant protein (Figure 8H), which was then applied to cultured PC12 cells (1.5 mg/ml) in order to identify intracellular signaling event that is likely to associate with the neuronal protective effect of MANF. Using antibodies to phosphorylated signaling proteins, we found that protein kinase C phosphorylation was increased by MANF (Figure 8I). Western blotting and immunohistochemical assays also showed a significant reduction in PKC phosphorylation in SCA17 KI mouse cerebellum tissue (Figures 8J and S7A). However, this reduction could be attenuated by the expression of transgenic MANF (Figure 8J).

It has also been reported that prolonged treatment with PMA, a PKC modulator, could reduce PKC expression and phosphorylation (Freisewinkel et al., 1991; Ohigashi et al.,

1999). We intraperitoneally injected PMA into 3-month-old WT and SCA17 KI mice (0.15 mg/kg, once every 3 days) for 24 days and found that this prolonged treatment indeed reduced phosphorylation of PKC (Figure S7B) and could worsen the motor impairment of SCA17 KI mice (Figure S7C). Reduction in PKC signaling has recently been found to affect dendritic branches and morphology of cerebellar Purkinje cells in the mouse brain (Thomanetz et al., 2013). It would be interesting to see whether the overexpression of PKC is able to reduce Purkinje cell pathology in SCA17 mice. Thus, we injected adenoviral vector expressing PKCγ into the cerebellum of SCA17 KI mice at 5 months of age. We observed a significant increase in the number of Purkinje cells and dendritic branches in the injected cerebellum of SCA17 KI mice 3 weeks after injection (Figures 8K, 8L, and S7D). These findings identified PKC as a downstream component of MANF-mediated signaling pathway and also highlighted the importance of PKC phosphorylation on the survival of adult Purkinje cells in SCA17.

DISCUSSION

Although aging is a primary risk factor promoting neurodegeneration caused by misfolded proteins, differentiating the cumulative effects of misfolded proteins on neurons over time versus aging-related factors that may make neurons vulnerable to misfolded proteins has proved difficult. Using our inducible SCA17 mouse model, we provide convincing evidence that aged neuronal cells are more vulnerable to misfolded proteins and that this vulnerability is related to the age-dependent decline in chaperone activity. Furthermore, we found that mutant TBP affects MANF expression and PKC signaling in Purkinje cells, which suggests a different pathogenic pathway in SCA17.

Strong evidence for the above idea comes from TBP105Q inducible KI mice expressing mutant TBP at the endogenous level for the same length of time: it is older KI mice that develop earlier and more progressive neurological phenotypes as well as more severe degeneration of cerebellar Purkinje neurons. However, the protein levels are determined not only by the time of synthesis but also by degradation. We found that more soluble mutant TBP was present in older KI mouse brains than the younger KI mouse brains, suggesting that mutant TBP is more stable in older neurons. A decreased cellular capacity to clear misfolded proteins by the UPS is seen in different brain regions and different types of cells (Keller et al., 2000), which could account for the increased levels of mutant proteins. However, this increased level is unlikely to be the sole determinant of selective neurodegeneration, given that mutant TBP is increased to a greater degree in the cortex than in the cerebellum, whereas it causes degeneration of Purkinje cells in the cerebellum. Thus, other cell-type-specific and aging-related factors must be involved in the selective neurodegeneration.

We identified MANF as a cell-type-specific target for Purkinje cell degeneration in SCA17. MANF is a newly discovered, noncanonical neurotrophic factor. Unlike other classical neurotrophins, such as NGF, BDNF, and NT-3, which mainly function by binding to their respective receptors in the cell membrane, MANF is believed to exert its neuroprotective effects both extracellularly, through binding to a currently unidentified receptor (Voutilainen et al., 2009), and intracellularly, by inhibiting apoptosis (Hellman et al., 2011). We provide

several lines of evidence to support the idea that MANF is involved in the selective Purkinje cell degeneration in SCA17. First, MANF is enriched in Purkinje cells, and its expression is reduced in SCA17 mouse cerebellum. Second, as a neuronal protective factor, the overexpression of MANF can alleviate Purkinje cell degeneration in SCA17 KI mouse brains. Third, the expansion of polyQ repeats reduces TBP binding to XBP1s and decreases the association of XBP1s to the promoter of MANF, resulting in decreased expression of MANF. Finally, we found that MANF could increase PKC phosphorylation in the cerebellum of SCA17 mice. Because TBP level is strictly regulated and the increased levels of mutant TBP can reduce the level of normal TBP, both the lower level of normal TBP and the dysfunction of mutant TBP can contribute to the decreased level of MANF via a similar mechanism of loss of function reported in other polyQ diseases (Lim et al., 2008; Nedelsky et al., 2010), resulting in impaired function of MANF in neuronal cells.

The signaling pathways mediated by MANF remain largely unclear. Using recombined MANF in PC12 cells, we found that MANF increased PKC phosphorylation. This finding led us to uncover the significant reduction of PKC phosphorylation in the cerebellum in SCA17 KI mice. Importantly, transgenic MANF can alleviate the reduction in PKC phosphorylation in SCA17 KI mouse cerebellum. Several studies indicate that PKC activity modulates Purkinje cell maturation, and reduction or absence of PKC signaling leads to abnormal Purkinje cell dendritic morphology and dysfunction during early development (Gundlfinger et al., 2003; Metzger and Kapfhammer, 2003; Thomanetz et al., 2013). PKC has complex effects, which are cell-type-dependent and different in developing neurons and adult neurons. It would be more important to understand whether and how PKC function is involved in the survival of Purkinje neurons in adult mice, given that SCA17 neuropathology occurs in adult neurons and that loss of PKC signaling has been found in the Purkinje cells of SCA1 mouse model (Skinner et al., 2001). In addition, PKCγ-null mice displayed impaired motor coordination (Chen et al., 1995). The importance of studying the role of PKC in adult neurons is also underscored by the fact that mutations in PKCγ can cause spinocerebellar ataxia 14, another age-dependent ataxia disease that is also characterized by cerebellar Purkinje cell degeneration (Chen et al., 2003; Shuvaev et al., 2011). Thus, decreased PKC activity mediated by loss of MANF could contribute to the late onset of Purkinje cell degeneration in SCA17.

Another important finding in our study is that an age-dependent decrease in Hsc70 contributes to age-dependent and selective neurodegeneration. Hsc70 is a constitutively expressed chaperone, which is different from other stress-induced chaperones, such as Hsp70 and Hsp40. Although both constitutive and inducible types of chaperones are thought to have similar effects on protein refolding and protection against neuronal damage, how they are related to the aging-related neurodegeneration process remains unclear. We found that Hsc70, but not Hsp40 or Hsp70, is selectively reduced in the brain with age. When a cell ages, senescing signals arise, typically as a result of DNA damage due to oxidative stress or telomere shortening. Regulation of the expression of constitutive chaperones may be more sensitive to aging-related oxidative damage than other inducible chaperones. The selective decrease of Hsc70 we see in the aged brain suggests that aging is more likely to affect the chaperoning function of unstressed neurons, which fits well with the slow and

progressive decline of cellular function for coping with misfolded proteins in the aged brains.

Hsc70 is also known to be involved in chaperone-mediated autophagy (CMA) by targeting proteins to lysosomes (Chiang et al., 1989). However, CMA activity is preserved in mice up to 12 months of age and could be upregulated by mutant polyQ proteins (Koga et al., 2011), so the decreased CMA function is unlikely to be involved in the neurotoxicity of mutant TBP in SCA17 KI mice younger than 12 months. In addition, mutant TBP is a nuclear protein whose turnover is unlikely to depend on the cytoplasmic CMA. Like other chaperones, Hsc70's critical function is to maintain protein folding and prevent their abnormal conformation and dysfunction or toxicity. Hsc70 is found to interact with cochaperones in order to maintain the conformation and interactions of protein complexes, such as DNA binding protein complex (Gehring, 2004; Li et al., 2008; Zeiner et al., 1999). Indeed, we found that the overexpression of Hsc70 can improve the association of mutant TBP with XBP1s and increase the transcription activity of the MANF promoter. Thus, a lower level of Hsc70 may impair the function of mutant TBP on the expression of MANF. Because MANF is enriched in Purkinje cells, this decrease can affect Purkinje cells in particular and contributes to the selective neurodegeneration in SCA17.

Our findings may have broad therapeutic implications for age-dependent neurodegenerative diseases. The effect of Hsc70 on mutant TBP's association with MANF suggests that improving this chaperone function can still effectively reduce mutant protein toxicity, even when mutant proteins have accumulated. Furthermore, we identified MANF as an additional target and PKC phosphorylation as its downstream signaling for SCA17 therapy. Because decreased levels in chaperone and MANF occur in old neurons, their function can be improved in the old age, which would be more economical than other preventative therapeutics that need to begin in earlier life. Given that Purkinje neuron degeneration is also prominent in other types of SCA diseases, the identification of MANF provides a potential target for the treatment of specific neurodegeneration in these diseases.

EXPERIMENTAL PROCEDURES

Antibodies and Plasmids

Antibodies and plasmids are described in the Supplemental Information.

Mouse Lines and Tamoxifen Injection

All mice were bred and maintained in the animal facility at Emory University under specific pathogen-free conditions in accordance with institutional guidelines of the Animal Care and Use Committee at Emory University. The TBP105Q floxed mice were generated as described previously (Huang et al., 2011). To generate TBP105Q inducible KI mice, we crossed heterozygous floxed TBP105Q mice with CreER transgenic mice (the Jackson Laboratory, B6.Cg-Tg[CAG-cre/Esr1]5Amc/J) that express tamoxifen-inducible Cre throughout the body. To generate germ-line KI (SCA17 KI) mice, we crossed heterozygous TBP105Q floxed mice with EIIa-Cre transgenic mice (the Jackson Laboratory, B6.FVB-Tg [EIIa-Cre] C5379Lmgd/J) in which Cre transgene under the control of the adenovirus EIIa

promoter is expressed in germline cells that transmit the genetic alteration to progeny. Primers were used for genotyping of the presence of mutant TBP (forward, 5′-CCA CAG CCT ATT CAG AAC ACC-3′; reverse, 5′-AGA AGC TGG TGT GGC AGG AGT GAT-3′) and Cre (forward, 5′-GCG GTC TGG CAG TAA AAA CTA TC-3′; reverse, 5′-TGT TTC ACT ATC CAG GTT ACG G-3′). To generate MANF transgenic mice, we inserted MANF cDNA linked with HA sequence into a previously described vector containing prion promoter (Friedman et al., 2007). The vector was sent to the Transgenic Mouse & Gene Targeting Core at Emory University for microinjection. Primers used for genotyping of transgenic MANF were forward, 5′-ATT GAC CTG AGC ACA GTG GAC CTG-3′; reverse, 5′-GTC ACT GTC ACC TTG TAC TCT GG-3′.

For the injection of tamoxifen into the mice, tamoxifen (Sigma-Aldrich, T5648) was dissolved in 100% ethanol to 10 mg/ml; corn oil (Sigma-Aldrich, C8267) was added and mixed thoroughly before ethanol was evaporated with Vacufuge plus (Eppendorf). Tamoxifen, dissolved in corn oil, was injected intraperitoneally into mice at 0.1 mg per 1 g body weight for 5 consecutive days.

For injection of Phorbol 12-myristate 13-acetate (PMA) into the mice, PMA (Sigma-Aldrich, P8139) was dissolved in corn oil and injected intraperitoneally into mice at the dose of 0.15 mg per 1 kg body weight every 3 days.

Mouse Behavior Tests

Mouse behavior tests were performed as described previously (Huang et al., 2011). Detailed procedures are provided in the Supplemental Information.

Cell Culture

Cell culture was performed as described previously (Shah et al., 2009). See also the Supplemental Information.

Viral Vector, Stereotaxic Injection, and Quantification of Neuronal Degeneration

Detailed procedures are described in the Supplemental Information.

Western Blot, Immunohistochemistry, and Immunoprecipitation

Methods were described previously (Huang et al., 2011). See also the Supplemental Information.

Luciferase Protection Assay

Assays were performed as described previously (Thulasiraman and Matts, 1998) with modifications (see the Supplemental Information).

RNA Expression and Promoter Transcriptional Activity Assay

Assays were performed as described previously (Friedman et al., 2007. See also the Supplemental Information.

Purification of Recombinant MANF Protein

This procedure is described in the Supplemental Information.

Statistical Analysis

For mouse behavioral analysis, each group consisted of at least six animals. For western blot analysis, immunostaining, or other biochemical assays, data were generated from three or more experiments, and the results were expressed as mean ± SEM. Statistical significances were calculated on the basis of a Student's t test, one-way ANOVA or two-way ANOVA, or a chi-square test. A p value < 0.05 was considered significant.

Supplementary Material

Refer to Web version on PubMed Central for supplementary material.

Acknowledgments

The work was supported by the National Institutes of Health (grants AG19206 and NS041669 to X.-J.L. and AG031153 and NS0405016 to S.L.). This research project was supported in part by the Viral Vector Core and the Emory University Integrated Cellular Imaging Microscopy Core of the Emory Neuroscience NINDS Core Facilities (grant P30NS055077) and the State Key Laboratory of Molecular Developmental Biology, China. We thank the Transgenic Mouse & Gene Targeting Core at Emory University for generating MANF transgenic mouse model. We thank Dr. David Ron for his generous contribution of XBP1u and XBP1s plasmids and Cheryl Strauss for critical reading of this manuscript.

REFERENCES

Afanas'ev I. Signaling and Damaging Functions of Free Radicals in Aging-Free Radical Theory, Hormesis, and TOR. Aging Dis. 2010; 1:75–88. [PubMed: 22396858]

Akerfelt M, Morimoto RI, Sistonen L. Heat shock factors: integrators of cell stress, development and lifespan. Nat. Rev. Mol. Cell Biol. 2010; 11:545–555. [PubMed: 20628411]

Bruni AC, Takahashi-Fujigasaki J, Maltecca F, Foncin JF, Servadio A, Casari G, D'Adamo P, Maletta R, Curcio SA, De Michele G, et al. Behavioral disorder, dementia, ataxia, and rigidity in a large family with TATA box-binding protein mutation. Arch. Neurol. 2004; 61:1314–1320. [PubMed: 15313853]

Cattaneo E, Zuccato C, Tartari M. Normal huntingtin function: an alternative approach to Huntington's disease. Nat. Rev. Neurosci. 2005; 6:919–930. [PubMed: 16288298]

Chen C, Kano M, Abeliovich A, Chen L, Bao S, Kim JJ, Hashimoto K, Thompson RF, Tonegawa S. Impaired motor coordination correlates with persistent multiple climbing fiber innervation in PKC gamma mutant mice. Cell. 1995; 83:1233–1242. [PubMed: 8548809]

Chen DH, Brkanac Z, Verlinde CL, Tan XJ, Bylenok L, Nochlin D, Matsushita M, Lipe H, Wolff J, Fernandez M, et al. Missense mutations in the regulatory domain of PKC gamma: a new mechanism for dominant nonepisodic cerebellar ataxia. Am. J. Hum. Genet. 2003; 72:839–849. [PubMed: 12644968]

Chiang HL, Terlecky SR, Plant CP, Dice JF. A role for a 70-kilodalton heat shock protein in lysosomal degradation of intracellular proteins. Science. 1989; 246:382–385. [PubMed: 2799391]

Freisewinkel I, Riethmacher D, Stabel S. Downregulation of protein kinase C-gamma is independent of a functional kinase domain. FEBS Lett. 1991; 280:262–266. [PubMed: 1901548]

Friedman MJ, Shah AG, Fang ZH, Ward EG, Warren ST, Li S, Li XJ. Polyglutamine domain modulates the TBP-TFIIB interaction: implications for its normal function and neurodegeneration. Nat. Neurosci. 2007; 10:1519–1528. [PubMed: 17994014]

Gehring U. Biological activities of HAP46/BAG-1. The HAP46/BAG-1 protein: regulator of HSP70 chaperones, DNA-binding protein and stimulator of transcription. EMBO Rep. 2004; 5:148–153. [PubMed: 14755308]

Gestwicki JE, Garza D. Protein quality control in neurodegenerative disease. Prog. Mol. Biol. Transl. Sci. 2012; 107:327–353. [PubMed: 22482455]

Gundlfinger A, Kapfhammer JP, Kruse F, Leitges M, Metzger F. Different regulation of Purkinje cell dendritic development in cerebellar slice cultures by protein kinase Calpha and -beta. J. Neurobiol. 2003; 57:95–109. [PubMed: 12973831]

Hellman M, Arumäe U, Yu LY, Lindholm P, Peränen J, Saarma M, Permi P. Mesencephalic astrocyte-derived neurotrophic factor (MANF) has a unique mechanism to rescue apoptotic neurons. J. Biol. Chem. 2011; 286:2675–2680. [PubMed: 21047780]

Henderson MJ, Richie CT, Airavaara M, Wang Y, Harvey BK. Mesencephalic astrocyte-derived neurotrophic factor (MANF) secretion and cell surface binding are modulated by KDEL receptors. J. Biol. Chem. 2013; 288:4209–4225. [PubMed: 23255601]

Hetz C. The unfolded protein response: controlling cell fate decisions under ER stress and beyond. Nat. Rev. Mol. Cell Biol. 2012; 13:89–102. [PubMed: 22251901]

Huang S, Ling JJ, Yang S, Li XJ, Li S. Neuronal expression of TATA box-binding protein containing expanded polyglutamine in knockin mice reduces chaperone protein response by impairing the function of nuclear factor-Y transcription factor. Brain. 2011; 134:1943–1958. [PubMed: 21705419]

Keller JN, Hanni KB, Markesbery WR. Possible involvement of proteasome inhibition in aging: implications for oxidative stress. Mech. Ageing Dev. 2000; 113:61–70. [PubMed: 10708250]

Koga H, Martinez-Vicente M, Arias E, Kaushik S, Sulzer D, Cuervo AM. Constitutive upregulation of chaperone-mediated autophagy in Huntington's disease. J. Neurosci. 2011; 31:18492–18505. [PubMed: 22171050]

Lee AH, Iwakoshi NN, Glimcher LH. XBP-1 regulates a subset of endoplasmic reticulum resident chaperone genes in the unfolded protein response. Mol. Cell. Biol. 2003; 23:7448–7459. [PubMed: 14559994]

Li XJ, Li S. Proteasomal dysfunction in aging and Huntington disease. Neurobiol. Dis. 2011; 43:4–8. [PubMed: 21145396]

Li L, Johnson LA, Dai-Ju JQ, Sandri-Goldin RM. Hsc70 focus formation at the periphery of HSV-1 transcription sites requires ICP27. PLoS ONE. 2008; 3:e1491. [PubMed: 18231578]

Lim J, Crespo-Barreto J, Jafar-Nejad P, Bowman AB, Richman R, Hill DE, Orr HT, Zoghbi HY. Opposing effects of polyglutamine expansion on native protein complexes contribute to SCA1. Nature. 2008; 452:713–718. [PubMed: 18337722]

Metzger F, Kapfhammer JP. Protein kinase C: its role in activity-dependent Purkinje cell dendritic development and plasticity. Cerebellum. 2003; 2:206–214. [PubMed: 14509570]

Mizobuchi N, Hoseki J, Kubota H, Toyokuni S, Nozaki J, Naitoh M, Koizumi A, Nagata K. ARMET is a soluble ER protein induced by the unfolded protein response via ERSE-II element. Cell Struct. Funct. 2007; 32:41–50. [PubMed: 17507765]

Nagai Y, Inui T, Popiel HA, Fujikake N, Hasegawa K, Urade Y, Goto Y, Naiki H, Toda T. A toxic monomeric conformer of the polyglutamine protein. Nat. Struct. Mol. Biol. 2007; 14:332–340. [PubMed: 17369839]

Nedelsky NB, Pennuto M, Smith RB, Palazzolo I, Moore J, Nie Z, Neale G, Taylor JP. Native functions of the androgen receptor are essential to pathogenesis in a Drosophila model of spinobulbar muscular atrophy. Neuron. 2010; 67:936–952. [PubMed: 20869592]

Ohigashi T, Mallia CS, McGary E, Scandurro AB, Rondon I, Fisher JW, Beckman BS. Protein kinase C alpha protein expression is necessary for sustained erythropoietin production in human hepatocellular carcinoma (Hep3B) cells exposed to hypoxia. Biochim. Biophys. Acta. 1999; 1450:109–118. [PubMed: 10354503]

Orr HT, Zoghbi HY. Trinucleotide repeat disorders. Annu. Rev. Neurosci. 2007; 30:575–621. [PubMed: 17417937]

Passos JF, von Zglinicki T. Mitochondria, telomeres and cell senescence. Exp. Gerontol. 2005; 40:466–472. [PubMed: 15963673]

Rolfs A, Koeppen AH, Bauer I, Bauer P, Buhlmann S, Topka H, Schöls L, Riess O. Clinical features and neuropathology of autosomal dominant spinocerebellar ataxia (SCA17). Ann. Neurol. 2003; 54:367–375. [PubMed: 12953269]

Shah AG, Friedman MJ, Huang S, Roberts M, Li XJ, Li S. Transcriptional dysregulation of TrkA associates with neurodegeneration in spinocerebellar ataxia type 17. Hum. Mol. Genet. 2009; 18:4141–4152. [PubMed: 19643914]

Shuvaev AN, Horiuchi H, Seki T, Goenawan H, Irie T, Iizuka A, Sakai N, Hirai H. Mutant PKCγ in spinocerebellar ataxia type 14 disrupts synapse elimination and long-term depression in Purkinje cells in vivo. J. Neurosci. 2011; 31:14324–14334. [PubMed: 21976518]

Skinner PJ, Vierra-Green CA, Clark HB, Zoghbi HY, Orr HT. Altered trafficking of membrane proteins in purkinje cells of SCA1 transgenic mice. Am. J. Pathol. 2001; 159:905–913. [PubMed: 11549583]

Takahashi T, Kikuchi S, Katada S, Nagai Y, Nishizawa M, Onodera O. Soluble polyglutamine oligomers formed prior to inclusion body formation are cytotoxic. Hum. Mol. Genet. 2008; 17:345–356. [PubMed: 17947294]

Thomanetz V, Angliker N, Cloëtta D, Lustenberger RM, Schweighauser M, Oliveri F, Suzuki N, Rüegg MA. Ablation of the mTORC2 component rictor in brain or Purkinje cells affects size and neuron morphology. J. Cell Biol. 2013; 201:293–308. [PubMed: 23569215]

Thulasiraman V, Matts RL. Luciferase renaturation assays of chaperones and chaperone antagonists. Methods Mol. Biol. 1998; 102:129–141. [PubMed: 9680615]

Toyoshima Y, Yamada M, Onodera O, Shimohata M, Inenaga C, Fujita N, Morita M, Tsuji S, Takahashi H. SCA17 homozygote showing Huntington's disease-like phenotype. Ann. Neurol. 2004; 55:281–286. [PubMed: 14755733]

Voutilainen MH, Bäck S, Pörsti E, Toppinen L, Lindgren L, Lindholm P, Peränen J, Saarma M, Tuominen RK. Mesencephalic astrocyte-derived neurotrophic factor is neurorestorative in rat model of Parkinson's disease. J. Neurosci. 2009; 29:9651–9659. [PubMed: 19641128]

Yoshida H, Matsui T, Yamamoto A, Okada T, Mori K. XBP1 mRNA is induced by ATF6 and spliced by IRE1 in response to ER stress to produce a highly active transcription factor. Cell. 2001; 107:881–891. [PubMed: 11779464]

Zeiner M, Niyaz Y, Gehring U. The hsp70-associating protein Hap46 binds to DNA and stimulates transcription. Proc. Natl. Acad. Sci. USA. 1999; 96:10194–10199. [PubMed: 10468585]

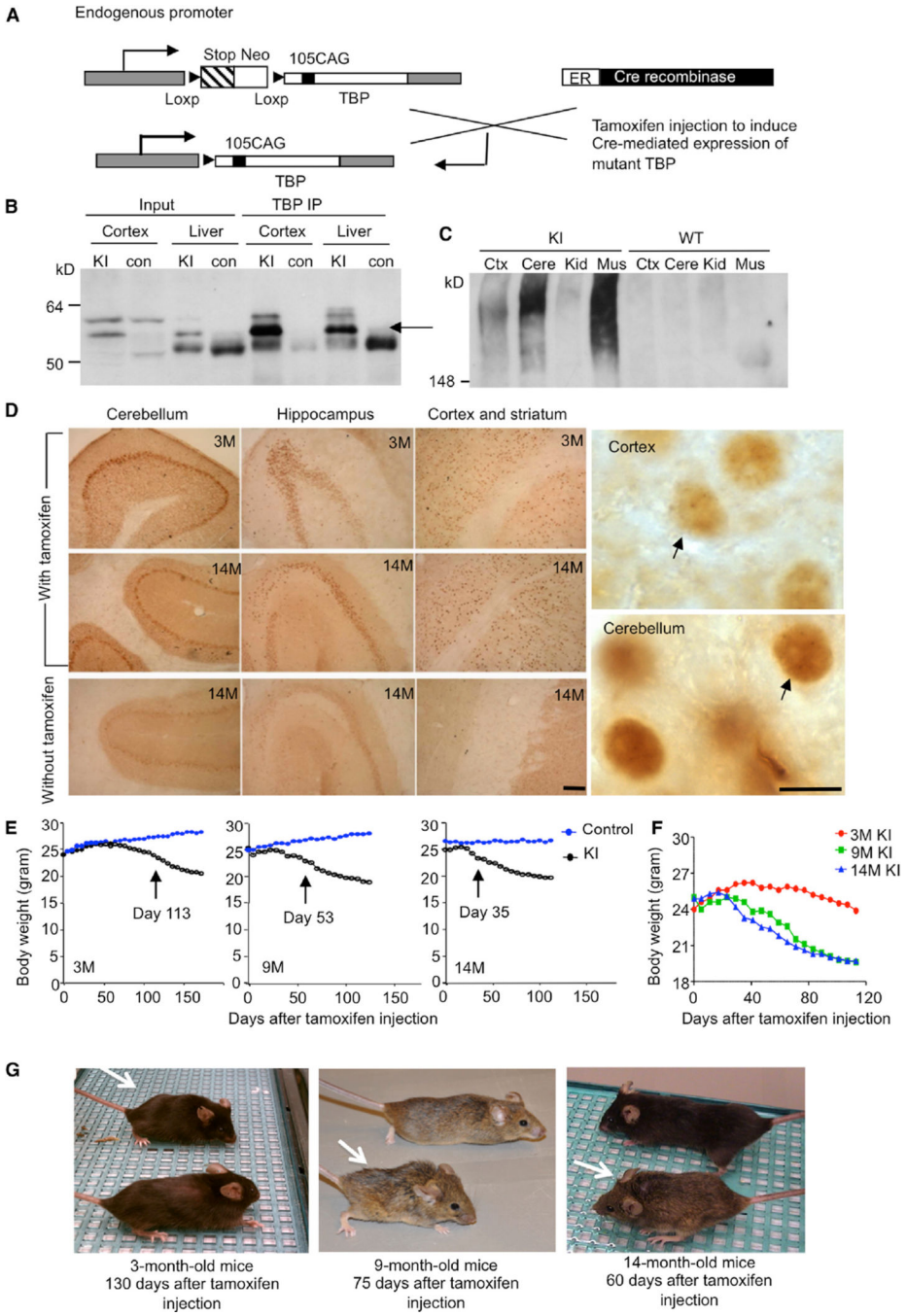

Figure 1. Characterization of TBP105Q Inducible KI Mouse Model

(A) A schematic illustration of expression of mutant TBP in TBP105Q inducible KI mice. (B) Western blotting analys is of immunoprecipitated TBP from the cortex and liver of WT and TBP105Q inducible KI mice after tamoxifen induction for two months. The rabbit polyclonal antibody EM192 was used to immunoprecipitate TBP, and the mouse monoclonal antibody 1C2 was used to visualize mutant TBP (arrow).

(C) Mutant TBP aggregates in the stacking gel were clearly detected in the cortex (Ctx), cerebellum (Cere), and muscle (Mus) of TBP105Q inducible KI mice by anti-TBP (1TBP18) but not in the kidney (Kid).
(D) 1C2 immunohistochemical study confirming mutant TBP expression in the cerebellum, hippocampus, cortex, and striatum of 3- and 14-month-old KI mice injected with tamoxifen. Small aggregates of mutant TBP were visualized in the nucleus under 1003 magnification (arrows). Scale bars represent 100 μm(left) and 5 μm (right).
(E) TBP105Q inducible KI and control mice at 3, 9, or 14 months of age were injected with tamoxifen in order to induce the expression of mutant TBP. The older KI mice showed earlier onset of body weight loss (day 35 for 14 months, $p = 0.0374$) than the younger KI mice (day 53 for 9 months, $p = 0.0125$, and day 113 for 3 months, $p = 0.0438$) after tamoxifen injection ($n = 9–11$ each group, two-way ANOVA, $p < 0.0001$).
(F) The body weight of differently aged KI mice was also compared.
(G) Representative images of differently aged (3, 9, and 14 months) KI mice (white arrow) were taken at the indicated days after tamoxifen injection.

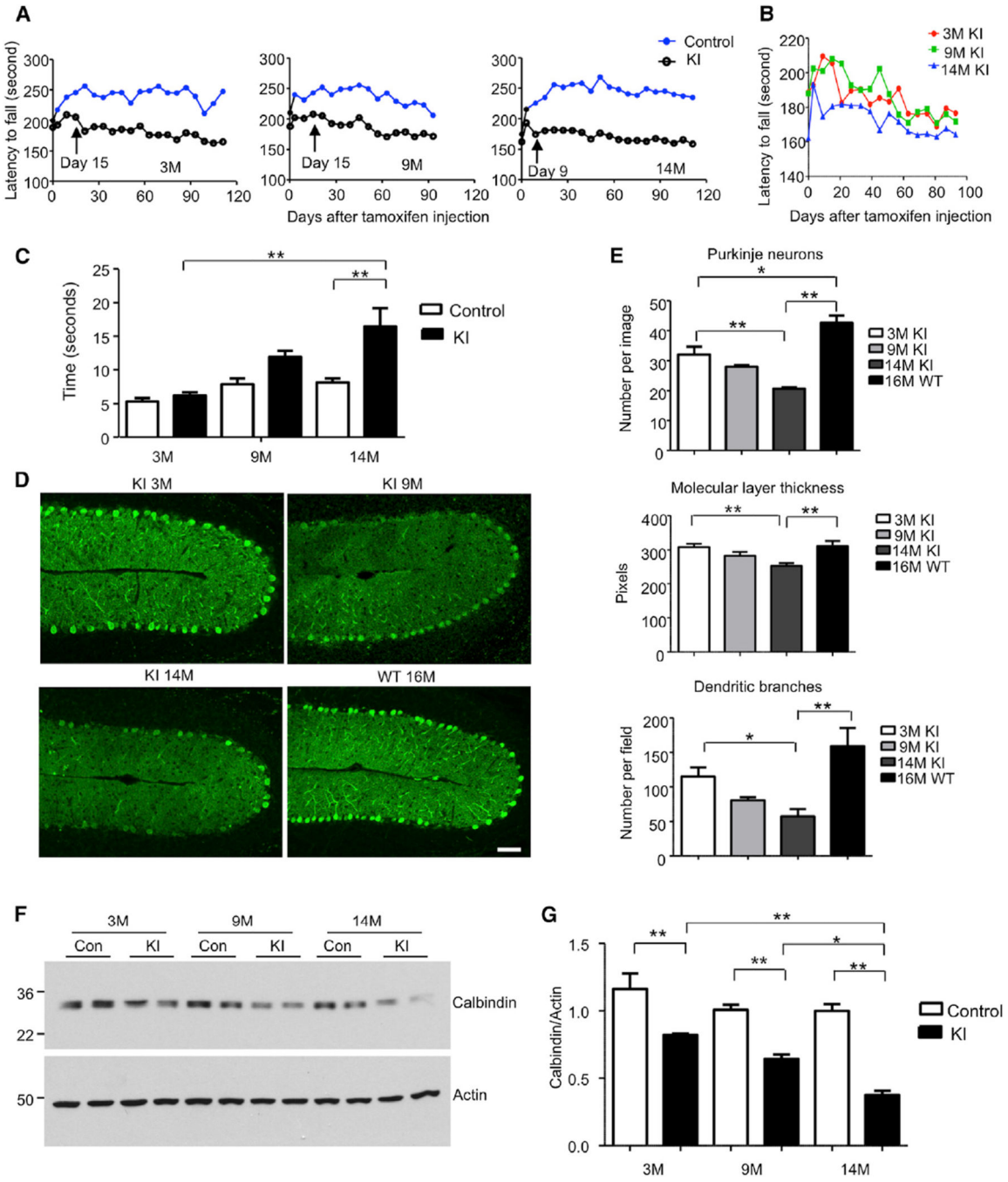

Figure 2. Aging Exacerbates Neurological Phenotypes in TBP105Q Inducible KI Mouse Model

(A) Motor activity of mice injected with tamoxifen at 3, 9, and 14 months of age was analyzed by rotarod test. The older KI mice (day 9 for 14 months, $p = 0.0031$) showed earlier on set of motor impairment than the younger KI mice (day 15 for 9 months, $p = 0.0298$, and day 15 for 3 months, $p = 0.0217$) after tamoxifen injection ($n = 9–11$ each group, two-way ANOVA, $p < 0.0001$).

(B) The rotarod performance of differently aged KI mice was also compared.

(C) Motor coordination of mice was tested by balance beam walking assay 1.5 months after tamoxifen injection. The walking time of older TBP105Q inducible KI mice on the beam is significantly longer than that of young KI mice ($n = 6$; $^{**}p < 0.01$).

(D) Degeneration of Purkinje neurons labeled by anticalbindin in the cerebellum of KI mice injected with tamoxifen at different ages. WT mouse at 16 months of age served as a control. The scale bar represents 50 μm.

(E) Quantification of Purkinje neuron number, molecular layer thickness, and dendritic branches in TBP105Q inducible KI mice at different ages ($n = 6–8$; $^{*}p < 0.05$, $^{**}p < 0.01$).

(F and G) Western blotting (F) and quantitative analysis (G) of calbindin protein level in the cerebellum of 3-, 9-, and 14-month-old TBP105Q inducible KI mice. Actin was used as a loading control ($^{*}p < 0.05$, $^{**}p < 0.01$). Data are represented as mean ± SEM.

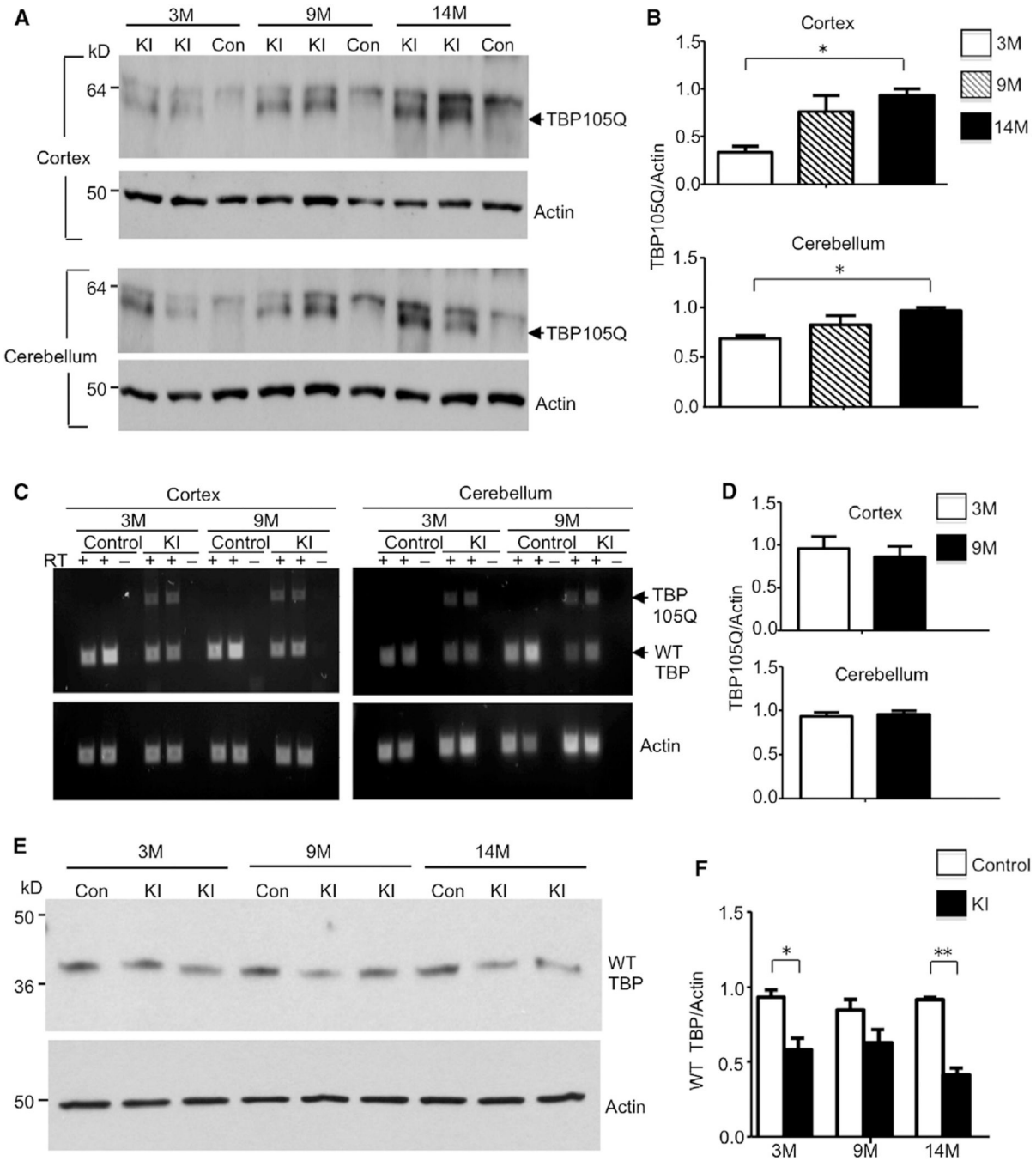

Figure 3. Age-Related Increase of Mutant TBP and Decrease of Wild-Type TBP in TBP105Q Inducible KI Mice

(A) Western blotting analysis of soluble mutant TBP levels in the cortex and cerebellum of 3-, 9-, and 14-month old TBP105Q inducible KI mice. An age-related increase of soluble mutant TBP (arrow) was observed in KI mice. Control mice (Con) did not show mutant TBP expression. Actin was used as a loading control.

(B) Quantification of the relative amount of TBP (the ratio of TBP to actin) on western blots (*$p < 0.05$).

(C) RT-PCR revealed similar mRNA levels of mutant TBP in both the cortex and cerebellum of 3- and 9-month-old TBP105Q inducible KI mice. Actin was used as an internal control.
(D) The ratio of mutant TBP to actin transcripts in RT-PCR is quantified.
(E) Western blotting analysis of the expression of mouse endogenous WT TBP in the cerebellum of TBP105Q inducible KI and WT mice at 3, 9, and 14 months of age.
(F) Quantitative analysis of WT TBP level on western blots by measurement of its ratio to actin (*$p < 0.05$, **$p < 0.01$). Data are represented as mean ± SEM.

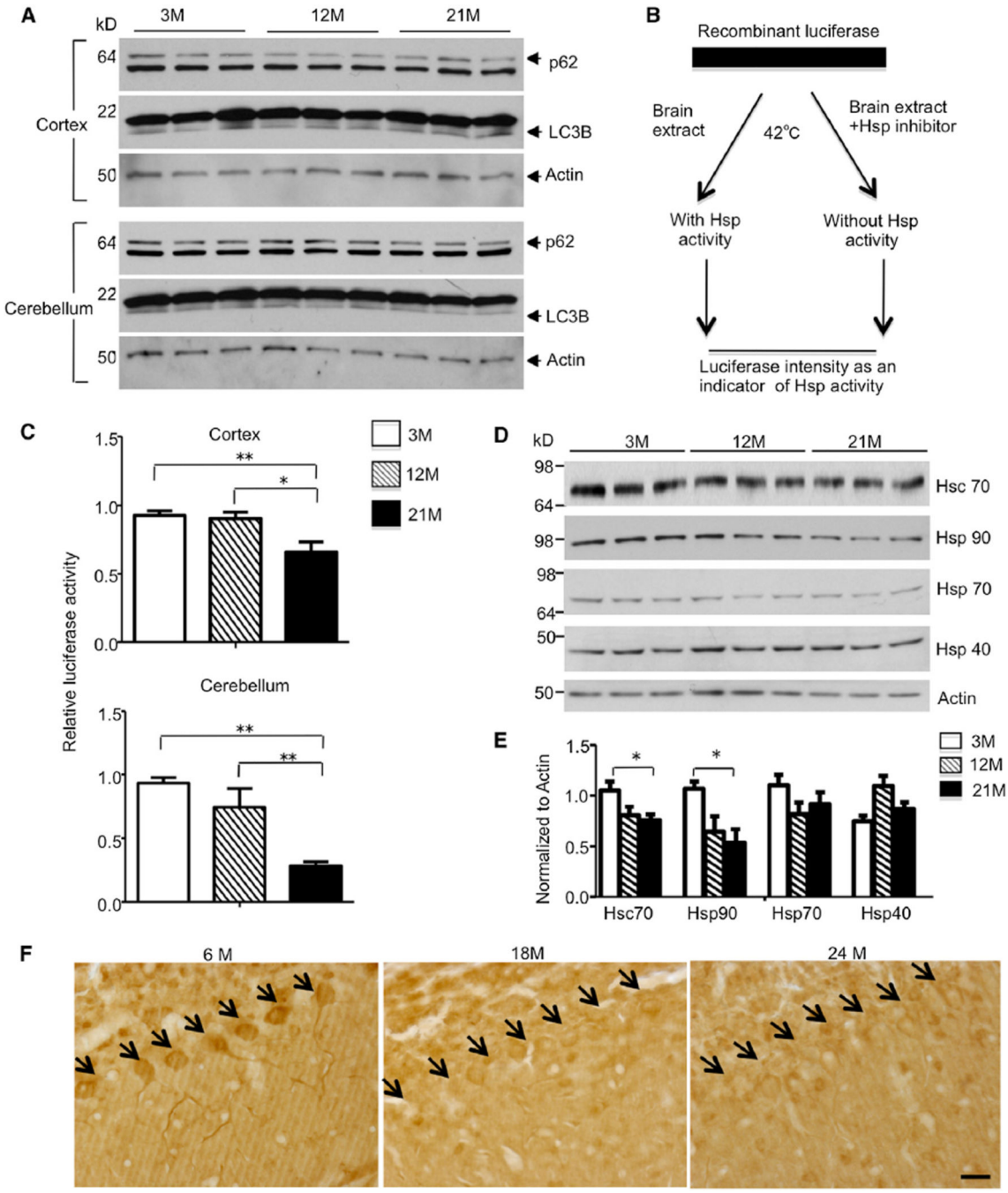

Figure 4. Age-Dependent Decrease in Chaperone Activity and Hsc70 Level in Mouse Brain

(A) Western blotting analysis of p62 and LC3B level in the cortex and cerebellum of 3-, 12-, and 21-month-old WT mice. No significant difference was found among three age groups.

(B) Luciferase protection assay was performed by incubating recombinant luciferase with lysates from either the cortex or cerebellum of 3-, 12-, and 21-month-old WT mice. Hsp inhibitor PU-H71 was added to the incubation in order to obtain Hsp-specific activity.

(C) Decreased luciferase intensity was observed when brain lysates of 12- or 21-month-old mice were used, indicating an age-related decrease of chaperone activity in the cortex and cerebellum (*$p < 0.05$, **$p < 0.01$).
(D) Western blot analysis of major chaperones with the cerebellum tissue from 3-, 12-, and 21-month-old WT mice. Actin was used as a loading control.
(E) The relative levels of Hsp were normalized by actin for quantification. Hsc70 and Hsp90 showed a significant decrease with aging (*$p < 0.05$, **$p < 0.01$).
(F) Hsc70 immunostaining showing age-dependent decrease in Hsc70 expression in Purkinje cells in WT mice at different ages (6, 18, and 24 months). Arrows indicate Purkinje cells. The scale bar represents 20 μm. Data are represented as mean ± SEM.

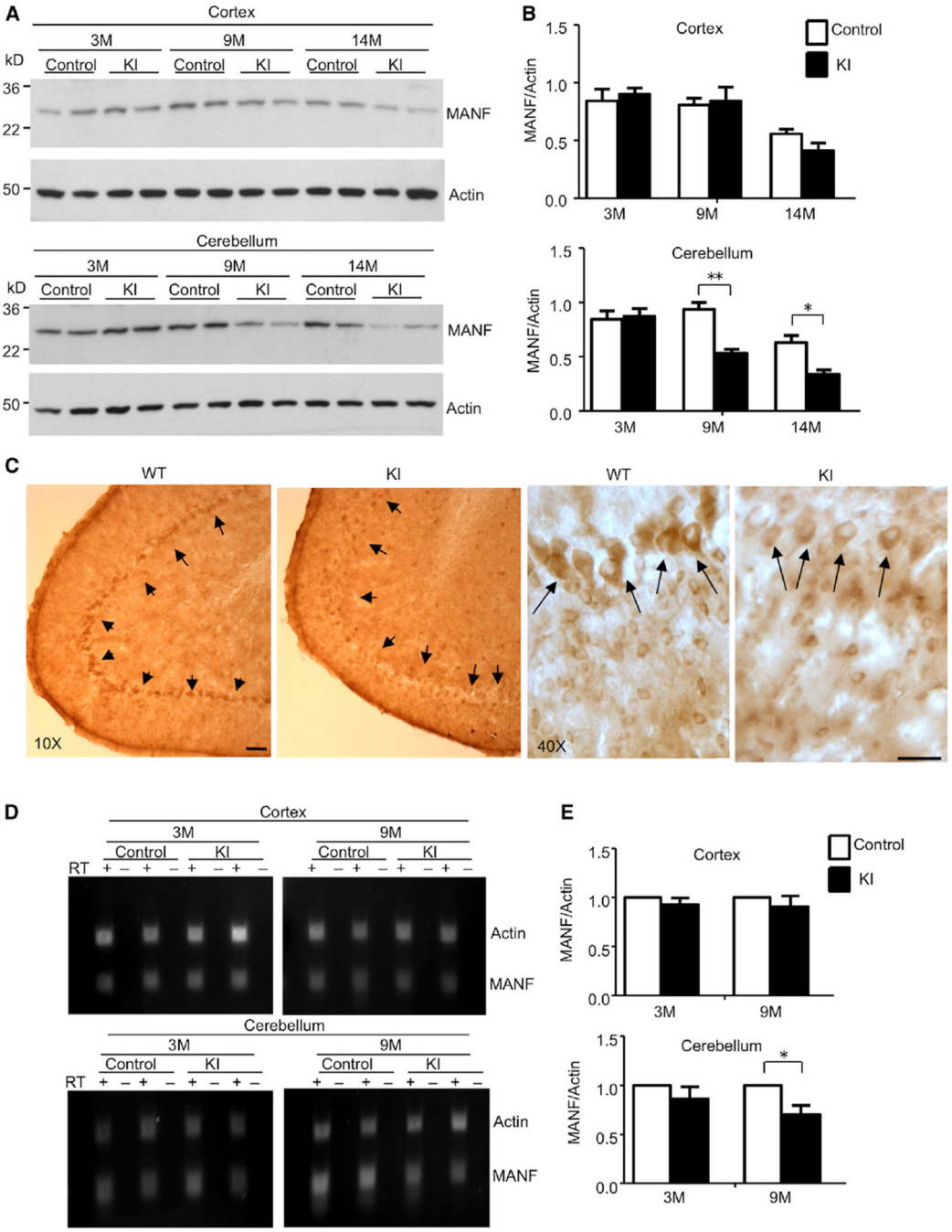

Figure 5. Decreased MANF Level in Purkinje Neurons of TBP105Q Inducible KI Mice

(A) Western blotting analysis of MANF protein level in the cortex and cerebellum of 3-, 9-, and 14-month-old control and TBP105Q inducible KI mice.

(B) Quantification of the ratio of MANF to actin showing that only the cerebellum in TBP105Q inducible KI mice, starting at 9 months, had a significant decrease of MANF in comparison to the control cerebellum (*$p < 0.05$, **$p < 0.01$).

(C) Immunohistochemical study showing the enrichment of MANF in Purkinje neurons of WT cerebellum, and this enrichment is lost in the cerebellum of 14-month-old TBP105Q inducible KI mouse. Scale bars represent 40 μm.
(D) RT-PCR revealed a decrease in MANF mRNA level, which is specific to the cerebellum of KI mice at an old age (9 months). Actin was used as an internal control.
(E) Real-time PCR was used to confirm the RT-PCR result. Relative abundance of MANF was calculated with the value from the control mice set to 1, and actin served as an internal control (*$p < 0.05$). Data are represented as mean ± SEM.

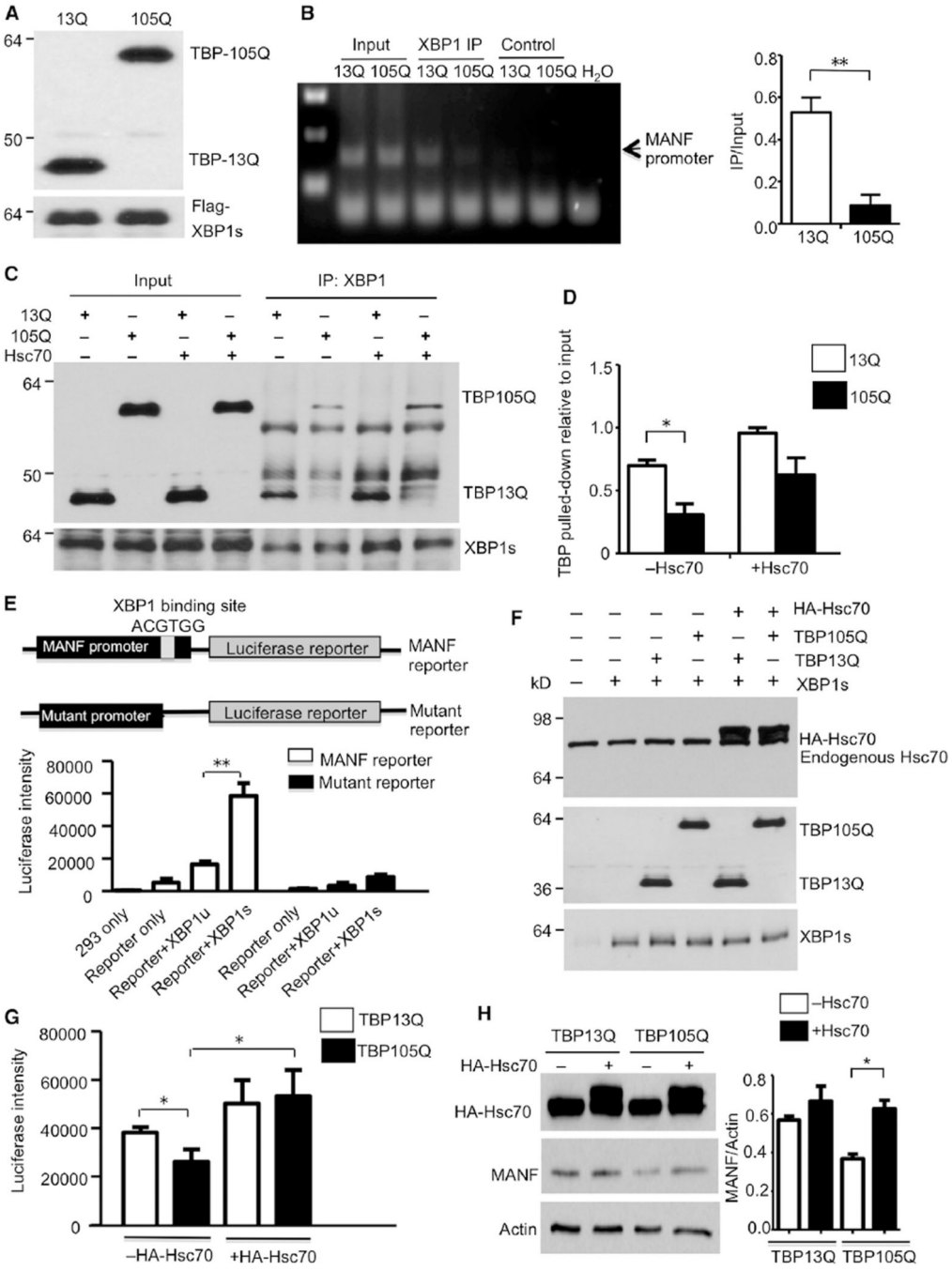

Figure 6. Expanded polyQ Impairs the Binding of TBP with XBP1s and Its Transcriptional Activity for MANF Expression

(A) Western blotting analysis confirmed the expression of respective proteins (TBP13Q, TBP105Q, and XBP1s) in cells used for ChIP assay.

(B) Semiquantitative PCR result using lysates from chromatin immunoprecipitation with anti-FLAG (ChIP, left). Control was beads only without anti-FLAG. More MANF promoter was pulled down in cells transfected with TBP13Q than with TBP105Q (right, $^{**}p < 0.01$).

(C) Coimmunoprecipitation of transfected XBP1s with TBP in the presence or absence of Hsc70. XBP1s was pulled down by XBP1 antibody in each sample, and less TBP105Q was

pulled down with XBP1s. Overexpression of Hsc70 increased the precipitated amount of TBP (both 13Q and 105Q).

(D) The relative amounts of TBP precipitated with XBP1s (*$p < 0.05$).

(E) Schematic map of luciferase constructs for reporter assay. Luciferase activity of transfected HEK293 cells showed that XBP1s, but not XBP1u, greatly increased luciferase intensity.

(F) Western blotting verifying the coexpression of TBP, Hsc70, and XBP1s with the MANF promoter reporter.

(G) Overexpression of Hsc70 significantly rescued the impaired luciferase activity by TBP105Q (*$p < 0.05$).

(H) Western blot analysis of MANF expression levels in TBP stably transfected cells that were transfected with (+) or without (−) HA-tagged Hsc70. The ratios of MANF to actin on the blot are also presented (*$p < 0.05$). Data are represented as mean ± SEM.

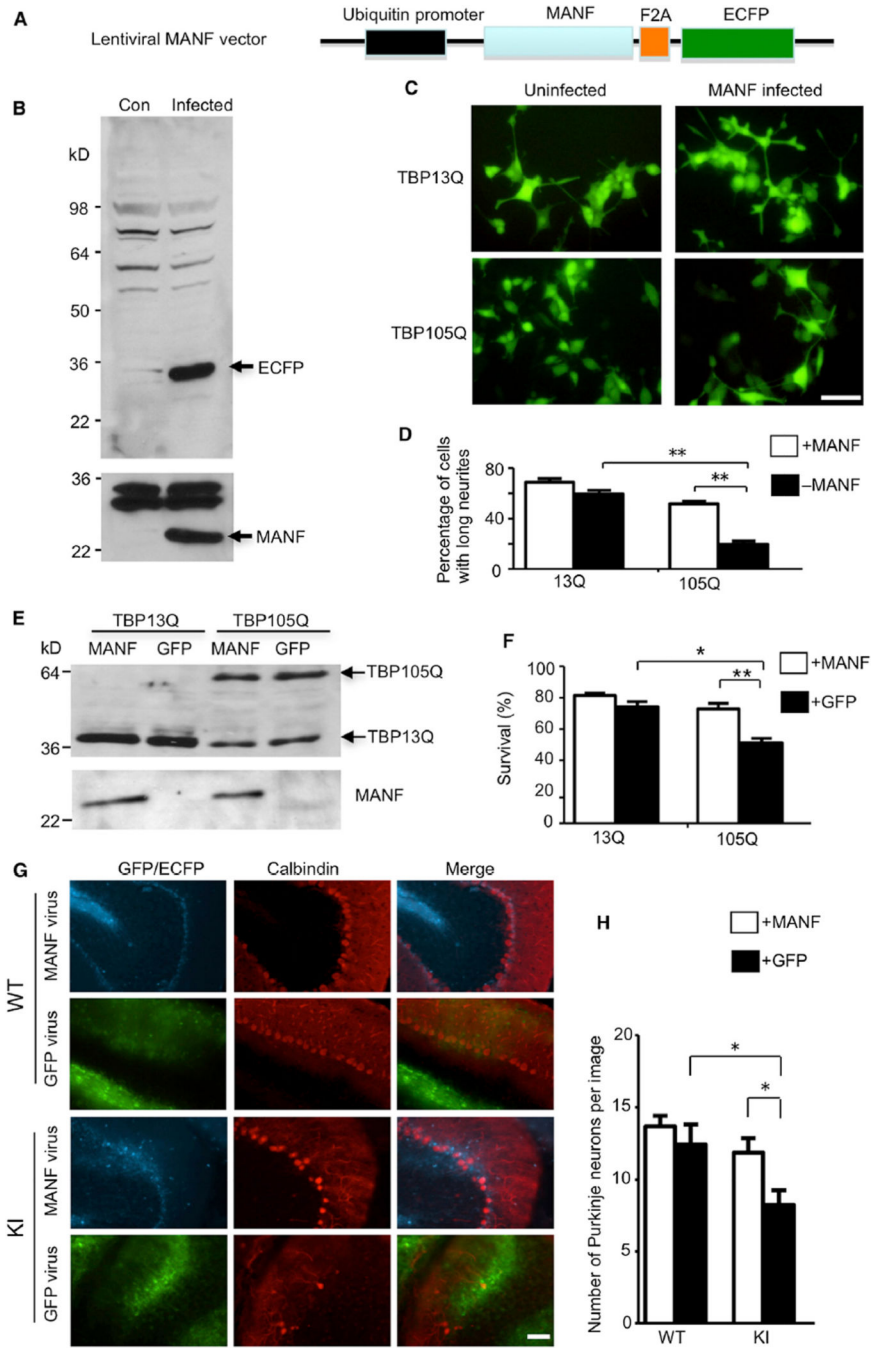

Figure 7. Overexpression of MANF Ameliorates Toxicity Caused by Mutant TBP In Vitro and In Vivo

(A) Schematic map of lentiviral MANF vector.

(B) Western blotting analysis of HEK293 cells infected with lentiviral MANF for two days (Infected) confirming the expression of both MANF and ECFP. Uninfected HEK293 cells (Con) were used as a negative control.

(C and D) PC12 cells stably expressing either WT TBP (TBP13Q) or mutant TBP (TBP105Q) were infected with lentiviral MANF or uninfected. Fluorescent imaging (C) and

quantitative analysis (D; n = 15, **p < 0.01) showed that MANF significantly increased the percentage of cells with long neurites. The scale bar represents 10 μm.

(E) Western blot analysis of PC12 cells stably expressing either WT TBP (TBP13Q) or mutant TBP (TBP105Q), which were infected with lentiviral MANF or GFP.

(F) MTS assay showed a significant increase in the survival of PC12 cells (versus non-staurosporine-treated cells) expressing mutant TBP when infected with lentiviral MANF in comparison to lentiviral GFP (*p < 0.05, **p < 0.01).

(G) One-year-old WT and TBP105Q inducible KI mice were injected with MANF lentivirus on the right side of the cerebellum and with lentiviral GFP on the left side. Fluorescence of GFP or ECFP was used to locate the region infected by lentivirus. Calbindin staining showed that MANF overexpression rescued the loss of Purkinje neurons caused by mutant TBP. The scale bar represents 50 μm.

(H) Quantitative assessment of the number of Purkinje cells labeled by anticalbindin per image field (20×, n = 9, *p < 0.05). Data are represented as mean ± SEM.

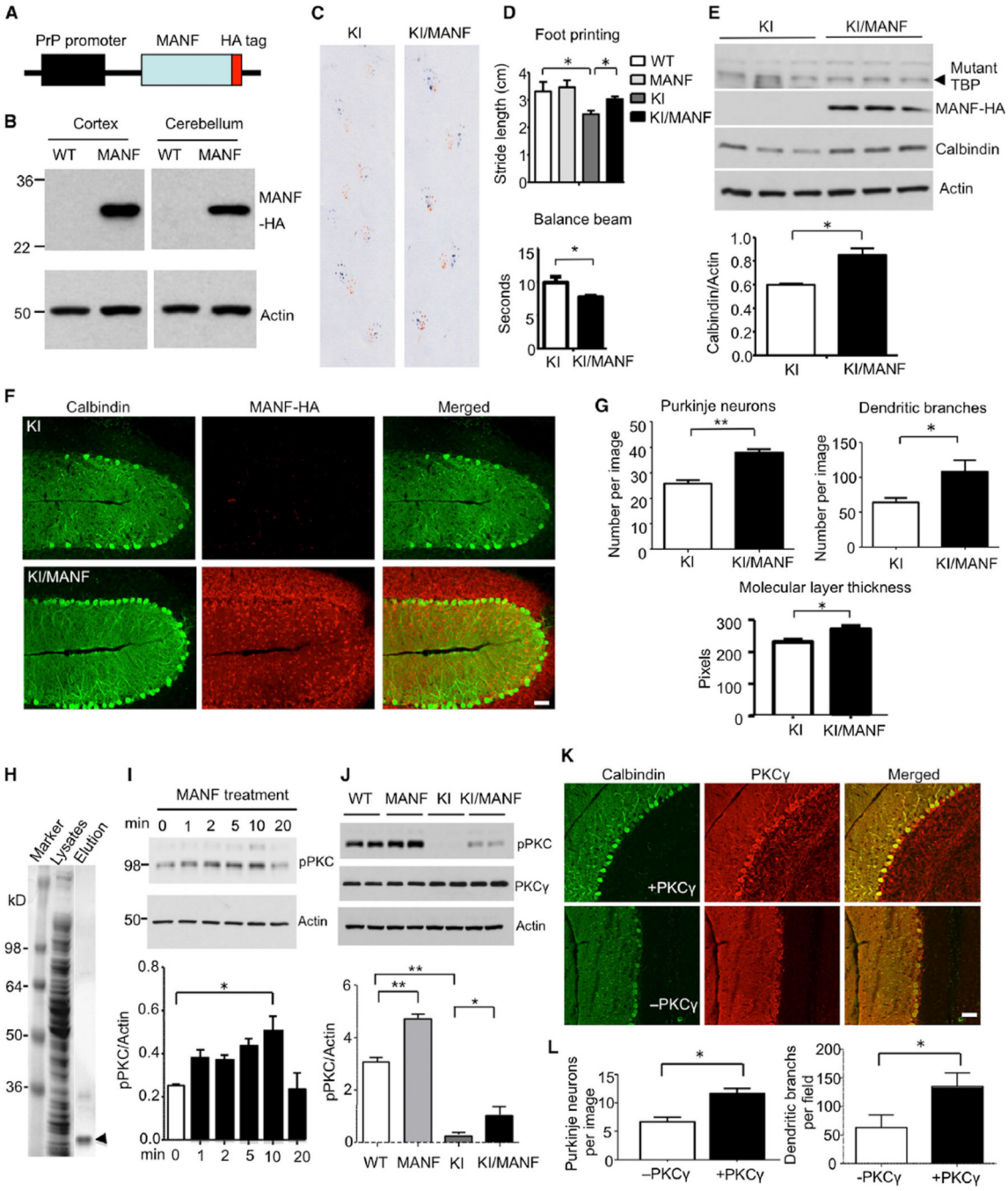

Figure 8. Expression of Transgenic MANF Ameliorates Pathological Phenotypes of SCA17 KI Mice via PKC Phosphorylation

(A) Schematic map of transgenic MANF construct.

(B) Anti-HA western blotting verified the expression of transgenic MANF-HA in the brain cortex and cerebellum in MANF transgenic mouse.

(C) Gait of SCA17 KI and KI/MANF mice was assessed with foot-printing assay.

(D) KI/MANF mice show longer stride lengths in foot-printing test and shorter walking time in balance beam assay than SCA17 KI mice, indicating an improvement in gait performance and motor coordination (n = 6 each group, *p < 0.05).

(E) Western blotting analysis of mutant TBP labeled by 1C2 antibody, transgenic MANF labeled by anti-HA, and calbindin in the cerebellum of 6-month-old SCA17 KI and KI/MANF mice. Actin was used as a loading control. The ratio of calbindin to actin is presented under the gel data (*$p < 0.05$).

(F) Immunofluorescent staining images (103 by confocal microscope) of SCA17 KI and KI/MANF mouse cerebellum. Calbindin staining was used to reveal Purkinje neurons, and HA antibody was used to stain transgenic MANF. The scale bar represents 50 μm.

(G) Quantitative assessment of the number of Purkinje neurons labeled by anticalbindin per image field, dendritic branches, and thickness of molecular layer (103, n = 9, *$p < 0.05$, **$p < 0.01$).

(H) Coomassie staining of SDS gel containing total bacterial lysates and eluted His-MANF (arrowhead).

(I) The purified His-MANF was applied to PC12 cells, and the PC12 cell lysates were collected 1, 2, 5, 10, and 20 min after MANF treatment and subjected to western blotting with an antibody to phosphor-PKC (pPKC). Actin was used as a loading control. The ratios of pPKC to actin are shown beneath the gel image (*$p < 0.05$).

(J) Western blotting analysis of pPKC and PKCγ in the cerebellum of mice with different genotypes. The ratios of pPKC to actin are show under the gel image (*$p < 0.05$, **$p < 0.01$).

(K) Immunofluorescent staining images of Purkinje neuron of SCA17 KI cerebellum injected with (+) or without (−) PKCγ adenovirus. Calbindin staining was used to reveal Purkinje neurons, and PKCγ antibody was used to detect viral PKCγ. The scale bar represents 50 μm.

(L) Quantitative analysis of the number of Purkinje cells and their branches in KI mice injected with or without viral PKCγ (20×, n = 9, *$p < 0.05$). Data are represented as mean ± SEM.